Journal of The Electrochemical Society, **155** (12) A875-A878 (2008)
0013-4651/2008/155(12)/A875/4/$23.00 © The Electrochemical Society

Performance Characteristics of Cathode Materials for Lithium-Ion Batteries: A Monte Carlo Strategy

S. Harinipriya, Vinten D. Diwakar,* and Venkat R. Subramanian,z**

Department of Chemical Engineering, Tennessee Technological University, Cookeville, Tennessee 38505, USA

A simulation strategy is formulated to study the performance of cathode materials in lithium-ion batteries. The methodology takes into account microscale properties, for example, diffusion of spherical electrode particle within the periodic boundary condition, $0 < x < l_p$. The electrode particles move in each step to its nearest-neighbor distance, employing the condition $ir(j) \geq \exp(-d\mathrm{Li}_1/ds)$, where "*ir*" represents the random number, $d\mathrm{Li}_1$ is the nearest-neighbor distance for the Li ion in the absence of solvent, and *ds* is the thickness of the solid phase. The Monte Carlo codes involve macroscale properties, namely, solvation effects, diffusion coefficients, and the concentration gradient to determine the diffusion of Li ions within the boundary conditions of $l_p < x < l_s$ and employing the random number criterion $ir(j) \geq \exp(-d\mathrm{Li}_1/ds)$, where $d\mathrm{Li}_1$ is the nearest-neighbor distance Li^+ can move in the presence of solvent and ds_2 is the thickness of the separator. The potential applied is in the range of 2.4–4.5 V and the capacity is calculated from the concentration of Li ions diffusing through the separator and the distance gradient. The discharge behavior for both $LiCoO_2$ and $LiFePO_4$ as cathode materials in lithium-ion batteries is in quantitative agreement with existing literature.

 [DOI: 10.1149/1.2976209]

Manuscript submitted March 20, 2008; revised manuscript received August 4, 2008. Published September 26, 2008.

Lithium-ion batteries are state-of-the-art power sources[1] for portable electronics. They combine excellent cycle life, no memory effect, and a high energy density.[2] The first commercially successful positive electrode[3] was $LiCoO_2$. However, the high cost of cobalt and potential safety hazards associated with the overcharging of $LiCoO_2$ forced the hunt for more stable material under abusive conditions. Lithium iron phosphate ($LiFePO_4$) is a potential cathode candidate for the next generation[4] of secondary lithium batteries due to its low cost, environment-friendly nature, cycling stability, and higher theoretical capacity of 170 mAh/g. However, the poor conductivity resulting from a low lithium-ion diffusion rate and low electronic conductivity in $LiFePO_4$ phase posed bottlenecks in their commercialization.[5-11] Several theoretical techniques such as mathematical modeling[12-15] and numerical analysis[16] are employed to optimize the performance of lithium-ion batteries. The working chemistries of $LiCoO_2$ and $LiFePO_4$ are different and hence make it difficult to devise an efficient single algorithm to investigate their performance as a cathode material. Because $LiFePO_4$ has more attractive properties as a cathode material than the commercial $LiCoO_2$, lithium transition metal phosphates with ordered-olivine structures, $LiMPO_4$ (M = Co, Ni, Mn, Fe), have attracted much attention as a promising cathode material for secondary lithium batteries.[17] The cycling capacity of $LiFePO_4$ is surprisingly good at low current densities or at elevated temperatures.[2,18,19] Lithium can be extracted from $LiFePO_4$ or inserted back into $FePO_4$ along a flat plateau[18] at 3.4 V vs Li. Increasing the current density does not lower the open-circuit potential,[18] but decreases its capacity. Padhi et al.[4] found that electrochemical extraction was limited to 0.6 Li/formula unit. They also suggested that the loss in capacity is because of lithium diffusion through the diminishing $LiFePO_4/FePO_4$ interface as lithium is reinserted into the structure. Goodenough et al.[4] suggested that a large amount of lithium could be extracted and reinserted reversibly in samples with smaller grain sizes. A multiscale and multistep kinetic Monte Carlo (MC) strategy is developed in the present work, which can predict the performance of both $LiFePO_4$ and $LiCoO_2$ by employing appropriate input parameters corresponding to each material. As an initial stage, the solvent interactions are taken into consideration via bonding energy between the carbonyl oxygen of the ethylene carbonate/diethyl carbonate (EC/DEC) mixture with the Li ions. In EC/DEC solvent, lithium ions are reported to hop between carbonyl oxygen bonds as $—C{=}O^{\delta-} \ldots Li^{\delta+}$ and hence solvent interaction is accounted for via Li–O partial bond formation. The discharge curves obtained agree satisfactorily with the existing literature for $LiCoO_2$ and $LiFePO_4$.

Methodology

The current methodology involved the assumption of the lithium-ion battery as depicted in Fig. 1. Cathode materials were $LiFePO_4$ and $LiCoO_2$ based on the case under consideration. The electrolyte employed was 1 M $LiPF_6$ in binary solvents EC/DEC in the ratio 1:1. Random numbers were generated to obtain the concentration of Li^+ that gets inserted in the cathode by employing appropriate diffusion coefficients and distance criteria. From the concentration variation and the distance the Li ions have diffused, the capacity of the discharge process, and state of discharge of the battery can be predicted. The lithium ion was allowed to diffuse by the formation and breaking of the $C{=}O^{\delta-} \ldots Li^{\delta+}$ bonds. It involved the hopping mechanism of Li ions in the solvent molecules to reach the destination electrode. Depending upon the ratio of the EC/DEC mixture assumed, the type of interaction between the Li ions and the solvent was varied to track the diffusion of the Li ions. The first MC simulation code included microscale properties such as the diffusion of spherical electrode particle within the periodic boundary conditions of $0 < x < l_p$. The electrode particles were assumed as spheres and allowed to move in each step only to a distance of its nearest neighbor, employing the condition $ir(j) \geq \exp(-d\mathrm{Li}_1/ds)$, where $d\mathrm{Li}_1$ was the nearest-neighbor distance for the Li ion in the absence of solvent and *ds* the thickness of the solid phase. The second MC code

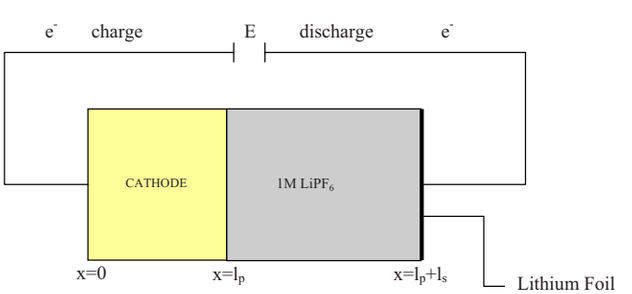

Figure 1. (Color online) Schematic representation of the lithium-ion cell assumed for the simulation purpose, cathode = $LiFePO_4$ or $LiCoO_2$, where "*x*" denotes the distance and the parameters l_p and l_s, represent the thickness (length) of cathode and separator, respectively.

* Electrochemical Society Student Member.
** Electrochemical Society Active Member.
z E-mail: vsubramanian@tntech.edu

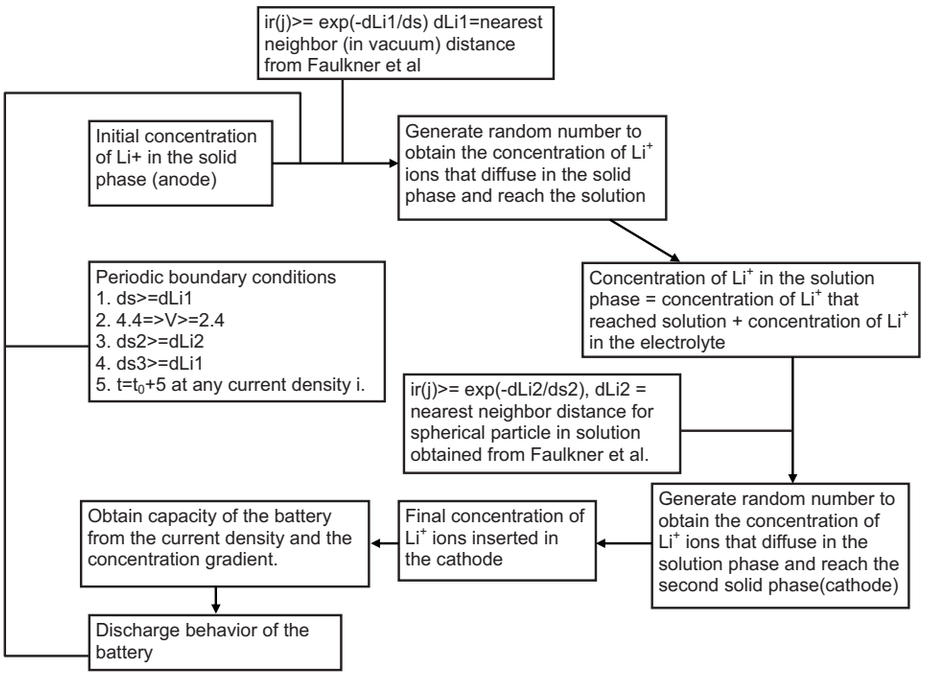

Scheme 1. The scheme for the proposed simulation methodology for the discharge behavior of $LiFePO_4$ and $LiCoO_2$ battery.

involved macroscale properties, namely, solvation effects, diffusion coefficients, and the concentration gradient to determine the diffusion of Li ions within the boundary conditions of $l_p < x < l_s$ and employing the random number criterion $ir(j) \geqslant \exp(-d\mathrm{Li}_1/ds)$, where $d\mathrm{Li}_1$ is the nearest-neighbor distance Li^+ can move in the presence of solvent and ds_2 the thickness of the separator. This MC strategy is schematically represented in Scheme 1. The potential applied was in the range of 2.4–4.5 V and the capacity was calculated from the concentration of Li ions diffusing through the separator and the distance gradient. Thus, the discharge behavior of $LiCoO_2$ and $LiFePO_4$ as electrode materials in Li-ion battery can be simulated from MC techniques employing different criteria. The present methodology helps in the reduction of computation time and employs basic molecular parameters to attain the result. MC seeds beyond 10^5 were not done because of convergence in the results from 10^2 to 10^5 seeds.

Parameters Employed

Input parameters for the MC simulation such as diffusion coefficient of Li ions in solid phase, solution phase, porosity of the electrode, particle size, solvent interaction energy, volume fraction of the active material due to insertion, and extraction of Li ions into the electrode are tabulated in Table I. The values for $LiFePO_4$ are taken from Srinivasan et al.[20] and $LiCoO_2$ are from Subramanian et al.[13-15]

Results and Discussion

The present MC simulation technique operates employing microscale properties such as the diffusion coefficient of lithium ions in a spherical electrode particle and the macroscale properties like solvation effects, the diffusion coefficient of lithium ion in the solution phase, and the concentration gradient to determine the number of Li ions diffusing in solution and the solid phase. The simulation codes are written in MATLAB version 6.5 and run on an Intel quad core personal computer. The computation time consumed to get the discharge profile for the system involving 23,800 moles of $LiFePO_4$ or $LiCoO_2$ at 10^5 MC seeds is approximately 20 h. The present simulation strategy can handle two different chemistries such as $LiFePO_4$ and $LiCoO_2$ as battery material without any difficulty. These diversifying results only need to consider input parameter variation corresponding to the material under investigation.

Discharge behavior of $LiCoO_2$.— Figures 2 and 3 indicate the discharge behavior of $LiCoO_2$/EC–DEC/Li half cell at different "*i*" values of 0.13, 0.26, 0.52, 1.3, 2.6, and 5.2 mA/cm^2 in time and capacity scales, respectively. Although the discharge starts at a common potential of around 4 V, at higher applied current densities the discharge rate is faster. This is consistent with the existing dynamic MC,[21] continuum models,[13-15] numerical analysis[16] in the literature for a given set of parameters employed. The maximum capacity attained by the half-cell $LiCoO_2$/EC–DEC/Li is 140 mAh/g and is in agreement with values in the literature.[15] Unlike $LiFePO_4$, $LiCoO_2$ does not undergo any phase transition during the discharge

Table I. The parameters employed in the simulation strategy for $LiCoO_2$ (Ref. 15) and $LiFePO_4$ (Ref. 20).

Parameters employed	Values
Design parameters	
Cathode thickness	62 μm
Porosity	0.25
Volume fraction of active material	0.347
Initial salt concentration	1 M
Separator thickness	25 μm
Particle size	43.3 nm
Electrode parameters	
Diffusion coefficient of Li in $LiFePO_4$	8×10^{-18} m^2/s
Diffusion coefficient of Li in $LiCoO_2$	1×10^{-14} m^2/s
Diffusion coefficient of Li in 1 M $LiPF_6$	7.5×10^{-10} m^2/s
Contact resistance	0.0065 Ωm^2
Solvent interaction energy	
Kinetic energy contribution	1 kT
Solvent interaction	$kT \times \log(N_{sol}/N_{tot})$
Total number of molecules, N_{tot}	23,800
Number of molecules in solvent, N_{sol}	Obtained from MC
Boltzmann constant, k	1.38×10^{-23} J/K
Temperature, T	298 K

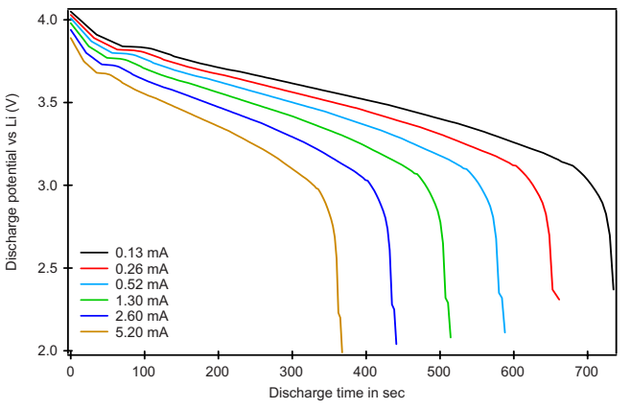

Figure 2. (Color online) The discharge behavior of (potential vs time) for $LiCoO_2$ (current applied in mA/cm^2).

process. Hence, a sudden drop in the capacity of the half-cell does not exist even at very high applied current densities, for example, 5.2 mA/cm^2. Scheme 2 represents the distribution of lithium ion in a CoO_2 structure during the discharge process. No phase transition exists during the Li insertion process and the distribution is gradual. The simulation results are given as an inset in Scheme 2 and the graphic is meant to describe the process via a simple pictorial representation. It can be inferred from this scheme and inset that, as the CoO_2 is getting lithiated or discharged, the lithium gets inserted into the lattice and a gradual decrease in the potential occurs with an increase in the concentration of Li in the lattice. At full discharge, the potential drops suddenly; here, the mole fraction of lithium (C_{Li} at that time/C_{Li} total) reaches unity, implying that the electrode is totally discharged. The concentration of Li at each time step is obtained from the MC codes and as a result the state of discharge is tracked.

Discharge behavior of LiFePO$_4$.— Figures 4 and 5 represent the discharge behavior of a $LiFePO_4$/EC–DEC/Li half cell at different applied current densities in time and capacity scale, respectively. It can be inferred from these figures that two distinct features exist: (*i*) decrease in the utilization[20,21] and (*ii*) decrease in the mid-plateau region with the increase in the applied current density.[20] The constancy of the potential over a wide range of time and capacity can be explained on the basis of a phase transition occurring during the insertion of Li into fully charged $FePO_4$. The constant behavior is mainly due to the equilibration of lithium deficient $Li_yFePO_4^{y-}$ and

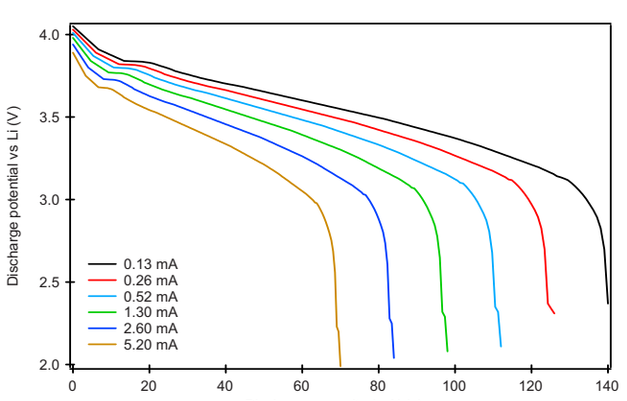

Figure 3. (Color online) The discharge behavior (potential vs capacity) for $LiCoO_2$ (current applied in mA/cm^2).

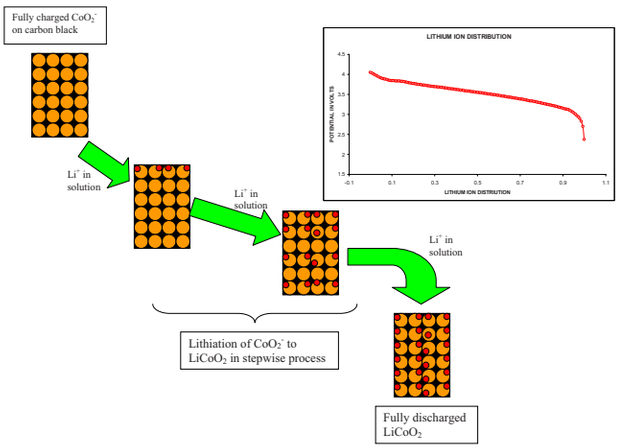

Scheme 2. Schematic representation of the processes occurring during discharge process of $LiCoO_2$ as lithium-ion battery cathode material; Li foil is employed as the anode and reference electrode for simulation purpose. Inset represents the discharge behavior of $LiCoO_2$ from simulations, identical with the results of Ref. 15.

lithium-rich $Li_{(1-x)}FePO_4^{(1-x)-}$ phases, on continuous discharging of the fully charged $FePO_4$. As seen in Scheme 3, the fully charged $LiFePO_4$ particle consists of a single $FePO_4$ phase. The discharge can be written as given by Srinivasan and Newman[20]

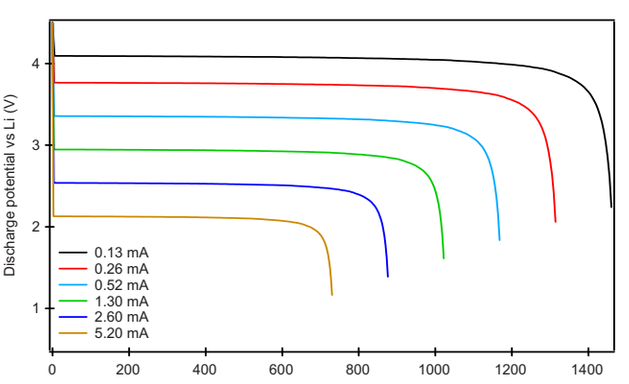

Figure 4. (Color online) The discharge behavior (potential vs time) for $LiFePO_4$ (current applied in mA/cm^2).

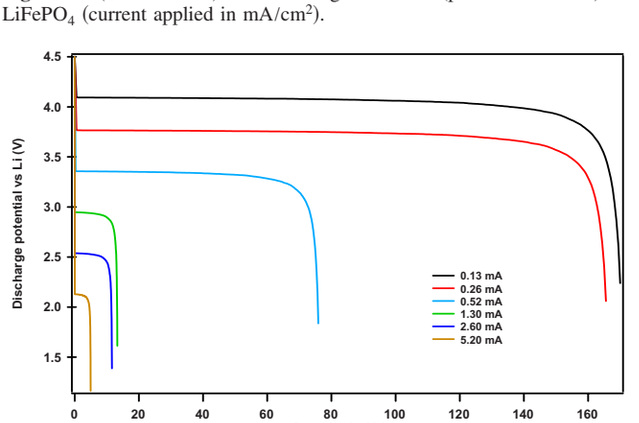

Figure 5. (Color online) The discharge behavior (potential vs capacity) for $LiFePO_4$ (current applied in mA/cm^2).

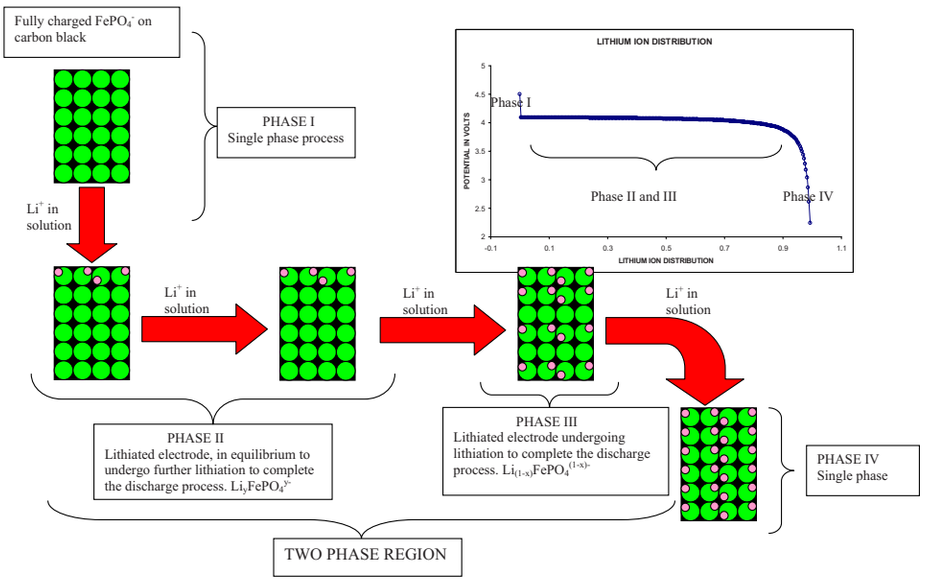

Scheme 3. Schematic representation of the processes occurring during discharge process of $LiFePO_4$ as lithium-ion battery cathode material; Li foil is employed as the anode and reference electrode for simulation purpose. Inset represents the discharge curve from simulation of results employing the above mechanism, identical with the results of Ref. 20.

$$FePO_4 + xLi^+ + xe^- \leftrightarrow xLiFePO_4 + (1 - x)FePO_4$$

and during the discharge process, the solid particles consist of two phases such as $FePO_4$ and $LiFePO_4$ in the proportion $(1 - x)$ and x respectively, "x" being the fraction of Li inserted into the solid particle of $FePO_4$. This first-order phase transition between the two species, $LiFePO_4$ and $FePO_4$, resists further lithiation of the cathode material, leading to constancy in the potential for a longer time and capacity window. As the applied current density increases, the time required for the equilibration of the two phases is reduced and hence a decrease in the mid-plateau region is noticed. Thus as "i" increases from 0.13 to 5.2 mA/cm^2 the capacity shows a drastic fall; this anomalous behavior could be attributed to the fact that the solvation energetic and the diffusion of Li ions in EC/DEC binary solvent play a vital role in the discharge process of $LiFePO_4$-based battery materials. Because Li hops by formation and breaking of the O–Li bond in consecutive steps, the increase in current density does not allow the process to occur efficiently, thereby leading to a sudden fall in the capacity. Thus, the present simulation methodology explains this well-known behavior of $LiFePO_4$ by employing simple random number criterion and periodic boundary conditions.

Perspectives

The simulation methodology presented here possesses a simple framework involving solvent interaction energetic, nearest-neighbor distance in solid and solvent, diffusion coefficient of Li ion in solid and solution phase in evaluating the performance of $LiCoO_2$ and $LiFePO_4$ as cathode materials by invoking the hard sphere validity assumptions in conjunction with solvent interactions and transport properties. Although existing MC simulation techniques can handle this issue very well, the inclusion of more input parameters to account for the conceptual background makes it computationally tedious, increases the computation time, and become specific to the chemistry of the material under investigation. However, we can reinstate that this MC strategy is complementary in nature to the extensive existing literature on lithium-ion battery and can easily be extended to understand the temperature effects on the battery performance, exact mechanism governing the nature of charge/discharge process, solvent interaction variations, conductivity profile of Li, and methods to improve the performance of the batteries.

Conclusions

The discharge behavior of $LiCoO_2$ and $LiFePO_4$ as cathode materials is in agreement with the existing literature in lithium-ion batteries. Current methodology is multiscale in nature by taking into account microscale properties such as the diffusion of spherical electrode particle within the periodic boundary conditions of $0 < x < l_p$ and macroscale properties such as solvation effects, diffusion coefficients, and the concentration gradient to determine the diffusion of Li ions within the boundary conditions of $l_p < x < l_s$. The potential applied is in the range of 2.4–4.5 V and the capacity is calculated from the concentration of Li ions diffusing through the separator and the distance gradient.

Acknowledgment

The authors acknowledge the U.S. Government for funding this work.

References

1. T. D. Hatchard, D. D. Macneil, A. Basu, and J. R. Dahn, *J. Electrochem. Soc.*, **148**, A755 (2001).
2. V. Srinivasan and C. Y. Wang, *J. Electrochem. Soc.*, **150**, A98 (2003).
3. K. Mizushima, P. C. Jones, P. C. Wiseman, and J. B. Goodenough, *Mater. Res. Bull.*, **15**, 783 (1980).
4. A. K. Padhi, K. S. Nanjundaswamy, and J. B. Goodenough, *J. Electrochem. Soc.*, **144**, 1188 (1997).
5. N. Ravert, Y. Chouinard, J. F. Magnan, S. Besner, M. Gauthier, and M. Armand, *J. Power Sources*, **97**, 503 (2001).
6. Z. Chen and J. R. Dahn, *J. Electrochem. Soc.*, **149**, A1184 (2002).
7. H. Huang, S. C. Yin, and L. F. Nazar, *Electrochem. Solid-State Lett.*, **4**, A170 (2001).
8. F. Croce, A. D'Epifanio, J. Hassoun, A. Deptula, T. Olczac, and B. Scrosati, *Electrochem. Solid-State Lett.*, **5**, A47 (2002).
9. S. Franger, F. Le Cras, C. Bourbon, and H. Rouault, *J. Power Sources*, **119**, 252 (2003).
10. S. Franger, F. Le Cras, C. Bourbon, and H. Rouault, *Electrochem. Solid-State Lett.*, **5**, A47 (2002).
11. S. Franger, C. Bourbon, and F. Le Cras, *J. Electrochem. Soc.*, **151**, A1024 (2004).
12. G. Ning, R. E. White, and B. N. Popov, *Electrochim. Acta*, **51**, 2012 (2006).
13. V. R. Subramanian, V. D. Diwakar, and D. Tapriyal, *J. Electrochem. Soc.*, **152**, A2002 (2005).
14. V. Boovaragavan and V. R. Subramanian, *J. Power Sources*, **173**, 1006 (2007).
15. V. R. Subramanian, V. Boovaragavan, and V. D. Diwakar, *Electrochem. Solid-State Lett.*, **10**, A255 (2007).
16. X.-C. Zhang, W. Shyy, and A. M. Sastry, *J. Electrochem. Soc.*, **154**, A910 (2007).
17. W. F. Howard and R. M. Spotnitz, *J. Power Sources*, **165**, 887 (2007).
18. V. Srinivasan and J. Newman, *Electrochem. Solid-State Lett.*, **9**, A110 (2006).
19. K. E. Thomas and J. Newman, *J. Electrochem. Soc.*, **150**, A176 (2003).
20. V. Srinivasan and J. Newman, *J. Electrochem. Soc.*, **151**, A1517 (2004).
21. R. Darling and J. Newman, *J. Electrochem. Soc.*, **146**, 3765 (1999).